Role of Solute Drag in Intestinal Transport

T. L. MULLEN, M. MULLER, and J. T. VAN BRUGGEN

From the Department of Biochemistry, Oregon Health Sciences University School of Medicine, Portland, Oregon 97201

ABSTRACT This study presents experiments related to the role of solvent drag and solute drag in the transmembrane movement of nonelectrolytes in a perfused rat intestine preparation. Conditions were chosen to simulate the effects of luminal hyperosmolarity on the permeability of tracer solutes. Data are presented on net water flux, transepithelial potentials, and lumen-to-blood and blood-to-lumen tracer solute movements during control electrolyte perfusion and after making the perfusate hyperosmotic. The results indicate that both solvent drag and solute drag can play significant roles in the transepithelial movement of solute and solute permeabilities in the rat ileum preparation. It is suggested that the potential roles of solvent drag and solute drag should be accounted for or considered during the characterization of the mechanisms of biological membrane function.

INTRODUCTION

The passive movement of nonelectrolytes across membranes cannot always be described by simple diffusion expressions because where there are transmembrane hydrostatic pressure or osmotic pressure gradients, there can be coupling of solute and solvent flows (solvent drag), and where there are transmembrane concentration gradients, there can be coupling of solute flows (solute drag). It is also possible that solute being carried by solvent drag, or by cotransport, can also interact with other solutes. According to the solute drag model proposed by Van Bruggen and co-workers (14, 16, 39, 40), the net flow of a hyperosmotic solute (driver) down its concentration gradient may significantly influence the movement of a second solute (tracer) by providing a vectorial force through physical collisions within the pores of the membrane. The phenomenon of solute drag has been studied extensively in heteropore and homopore artificial membranes. It has been established (16, 39) that solute-solute interaction increases with increasing molecular size of both the hyperosmotic agent and the tracer solute, with increasing concentration of the hyperosmotic agent, and with decreasing membrane pore diameter.

Address reprint requests to Dr. Terry Mullen, Dept. of Biology, Western State College of Colorado, Gunnison, CO 81230.

J. GEN. PHYSIOL. © The Rockefeller University Press · 0022-1295/85/03/0347/17 $1.00

Volume 85 March 1985 347–363

Electrophysiological studies (6, 31, 41) have revealed a high conductance shunt pathway across leaky epithelia, and it has been concluded (24, 25, 38, 42) that the tight junctions and lateral extracellular spaces make up the anatomical counterpart of the electrical shunt. Permeability studies (3, 13, 20) reveal that the pathway provides an aqueous environment for the diffusion of small solutes and has an effective pore diameter of ~5–35 Å. Since solute drag across artificial membranes does take place with solutes of physiological importance, it would seem likely that solute drag through the paracellular shunt is a force in biological transport.

Anomalous transport of nonelectrolytes has been reported in amphibian skin (4, 14, 15, 36) and bladder (21) exposed to external hyperosmolality with a net flux of solute against the net flow of water. The apical or mucosal surfaces of these amphibian epithelia are, however, naturally exposed to a hypoosmotic environment, and thus the demonstration of a significant solute drag effect probably has little adaptive or physiological significance. The gastrointestinal tract of man, on the other hand, is presented with a great variety of solutions with widely varying osmolality and chemical composition (1, 26). By analogy to the studies on artificial membranes in the gastrointestinal tract, solute drag could be of physiological significance in biological transport since large transepithelial concentration gradients do occur. There is abundant evidence for the coupling of a number of flows across the intestine, i.e., sugar transport is coupled to Na transport (5, 32), amino acid transport is coupled to Na transport (7, 32), Cl transport is coupled to Na transport (27, 29), and salt transport is coupled to water transport (11).

We have attempted to determine if solute drag could contribute to the flux of solute across the gastrointestinal tract of the rat under conditions close to physiological. We used an in vivo preparation similar to that employed by Curran and Solomon (8) and Humphreys (18). We have studied the effect of the hyperosmotic drivers urea, mannitol, and polyethyleneglycol (PEG) 600 on the flux and permeability of the tracer solutes urea and erythritol across the in vivo rat ileum.

At the onset of our studies, it was known that there were a number of factors of differing magnitudes, in addition to solute drag, that could influence solute diffusion and absorption. Some of the forces that may modify solute diffusion across membranes are: solvent drag (metabolic or osmotically induced), unstirred layers (which may be especially significant in the intestinal segment system) (9, 10), modification of unstirred layer effects both by solvent flow and solute drag, and pore size changes with bathing solution modification. The reflection coefficient is a quantitative reflection of pore size. Although not all of these variables can be quantitated or controlled separately, their cumulative effect on tracer diffusion across the gastrointestinal tract can be measured. In order to demonstrate the influence of the driver solute on the diffusion of the tracer solute, solute drag, the approximate magnitude of the cited force was considered. These studies indicate that the force, solute drag, as well as solvent drag, should be considered in descriptions of the factors influencing "passive transport" of solutes across the gastrointestinal tract under physiological conditions.

MATERIALS AND METHODS

General Procedure

Studies were performed on 80 female Sprague-Dawley rats weighing 326 ± 4 g, which were fasted for 24 h before the experiment but were allowed free access to water. The animals were anesthetized with an intraperitoneal injection of Inactin (Andrew Lockwood & Assoc., East Lansing, MI; 120 mg/kg body weight). The rectal temperatures were monitored via a thermister probe (model YSI 423, Yellow Springs Instrument Co., Yellow Springs, OH) connected to a polygraph (model 70, Grass Instrument Co., Quincy, MA), and the body temperatures were maintained at 37°C by the use of a heat lamp. After a tracheotomy was performed, one polyethylene catheter (PE 50) was placed in the jugular vein for the infusion of fluid, and another was placed in the carotid artery for the collection of blood samples and for the recording of blood pressure via a strain gauge (model P23AC, Gould Instrument Co., Oxnard, CA) connected to a polygraph. The abdomen was opened along the midline, and a 20-cm segment of jejunum (just distal to the ligament of Treitz), ileum (proximal to the ileocecal junction), or colon (5 cm) was located. A small incision was made in the antimesenteric borders at each end of the selected segment, and intestinal contents were removed by gentle irrigation with 10–20 ml of normal electrolyte solution with the following composition (mM): 119 NaCl, 21 $NaHCO_3$, 2.4 K_2HPO_4, 1.2 $CaCl_2$, 1.2 $MgCl_2$, 0.6 KH_2PO_4, with a pH of 7.4 at 37°C when gassed with 95% O_2/5% CO_2. Polyethylene catheters (PE 240 at the proximal end and PE 350 at the distal end) were then placed in the segment so as not to interfere with the normal blood supply, and the irrigation procedure was repeated. A sustaining intravenous infusion of normal electrolyte solution was delivered throughout all control experiments at a rate of 20 μl/min by a constant-infusion pump (model 975, Harvard Apparatus Co., Inc., South Natick, MA).

The transepithelial potential difference (TEP) (blood side positive) was measured across the perfused segment using matched Ag/AgCl bioelectrodes. One was connected to the perfusion fluid via an agar bridge inserted in the perfusion line close to the segment, and the other was placed in a beaker of normal electrolyte solution into which the cut tip of the rat's tail was immersed. The TEP was recorded continuously on a recorder (model 2541, Brinkmann Instruments, Inc., Westbury, NY). Arterial blood samples (1.5 ml) were collected every 64 min from a three-way valve connected to the carotid catheter; this volume was immediately replaced with stock solution. The osmolalities of plasma, perfusate, and effluent samples were determined with a freezing point osmometer. When appropriate, urea concentrations were determined by the carbamino-diacetyl reaction method as adapted to an autoanalyzer (Technicon Instruments Corp., Tarrytown, NY).

Samples were assayed for ^{14}C and ^{3}H in a liquid scintillation spectrometer (model 2425, Packard Instrument Co., Inc., Downers Grove, IL) with appropriate corrections for quenching and background (external standards method). Disintegrations per minute (dpm) were calculated from the assay of 0.5-ml aliquots of the intestinal effluent or on 0.1 ml of plasma. Permeability values are reported only for intervals where a steady state was shown to have been achieved. Values are expressed as means ± SE. The *t* test was used to test for differences between means at the 5% probability level or below. In the appropriate tables, the difference between the means is cited as significant (S) or not significant (NS).

Lumen-to-Blood Permeability

Intestinal segments were perfused at 37°C in the proximal-to-distal direction at a rate of 210 μl/min by a constant-infusion pump. Segments were perfused with a normal electrolyte solution for a 160-min control period followed by a hyperosmotic solution (control solution

made 100, 250, or 500 mM with urea, mannitol, or PEG 600). The hyperosmolar experimental period was 128 min. The presence of 500 mM solute in the luminal perfusate of the ileum and jejunum required an increase in volume of sustaining intravenous infusion from 20 to 39 μl/min in order to avoid dehydration of the animal. The entire intestinal effluent was collected in 16-min fractions, with the first two samples being discarded to allow for the attainment of steady state fluxes. Arterial blood samples were taken every 64 min to evaluate the degree of tracer backflux and were replaced with an equal volume of normal electrolyte solution.

[^{3}H]Inulin (10 μCi/100 ml) was added to the control and hyperosmotic perfusates as a nonadsorbed volume marker. The net flux of water ($J_{net}^{H_2O}$) was calculated from the difference in inulin concentration between the perfusate and effluent as follows:

$$J_{net}^{H_2O} = V_i \left[1 - \frac{(In)_p}{(In)_e}\right] \frac{60}{L}, \quad (1)$$

where $J_{net}^{H_2O}$ is the net flux of water in milliliters per centimeter per hour with a positive value indicating net water movement in the lumen-to-blood direction; V_i is the rate of intestinal perfusion in milliliters per minute; $(In)_p$ and $(In)_e$ are disintegrations per minute per milliliter of [^{3}H]inulin in the intestinal perfusate and effluent, respectively; and L is the length of the intestinal segment in centimeters.

In separate experiments, tracer solute diffusion was measured in the lumen-to-blood (l → b) or the blood-to-lumen (b → l) direction. The intestinal perfusates in the lumen-to-blood experiments contained 2 μCi/100 ml of [^{14}C]solute, 5 mM nonlabeled tracer material, and the inulin volume marker. This solution was perfused through a 20-cm segment of jejunum or ileum, or a 5-cm segment of colon at the rate of 210 μl/min. The permeability of the solute in the lumen-to-blood direction ($P_{l\to b}^s$) was calculated by the disappearance of labeled solute from the intestinal perfusate as follows:

$$P_{l\to b}^s = \frac{V_i \left[(S)_p - \frac{(S)_e(In)_p}{(In)_e}\right]}{60\, L(S_m)_e}, \quad (2)$$

where $P_{l\to b}$ is the permeability coefficient of solute in the lumen-to-blood direction in square centimeters per second; $(S)_p$ and $(S)_e$ are disintegrations per minute per milliliter of [^{14}C]solute in the intestinal perfusate and effluent, respectively; and $(S_m)_e$ is the disintegrations per minute per milliliter mean of the [^{14}C]solute in the perfusate and effluent, which is an approximation of the activity of the labeled solute in the gut.

Blood-to-Lumen Permeability

The stock solution containing the volume marker was perfused through a 5-cm intestinal segment at 300 μl/min in order to reduce tracer backflux. A 1-ml intravenous priming dose of [^{14}C]solute (8 μCi/ml) was given before starting the sustaining intravenous infusion, which contained 40 μCi/100 ml of [^{14}C]solute in stock solution. The replacement fluid injected after a blood sample was taken contained 6 μCi/100 ml [^{14}C]solute in stock solution. The apparent permeability of the solute in the blood-to-lumen direction ($P_{b\to l}^s$) was calculated from the appearance of labeled solute in the intestinal effluent as follows:

$$P_{b\to l}^s = \frac{V_i(S)_e(In)_p}{60\, L(S)_b(In)_e}, \quad (3)$$

where $P_{b\to l}^s$ is the permeability coefficient of solute in the blood-to-lumen direction in square centimeters per second, and $(S)_b$ is disintegrations per minute per milliliter of [^{14}C]solute in the blood.

Reflection Coefficient

According to Kedem and Katchalsky (19), the net flux of a solute (J^s_{net}) can be expressed by:

$$J^s_{net} = P^s_T \Delta C^s + (1 - \sigma^s) J^{H_2O}_{net} \bar{C}^s, \tag{4}$$

where P^s_T is the true (thermodynamic) permeability coefficient of the solute; ΔC^s is the concentration difference of solute across the barrier; σ^s is the reflection coefficient for solute; and $\bar{C}^s$ is the mean solute concentration across the barrier.

In the in vivo intestine, the unidirectional fluxes of tracer solute ($J^s_{l\to b}$ and $J^s_{b\to l}$) can be represented by:

$$J^s_{l\to b} = P^s_T C^s_l + (1 - \sigma^s) J^{H_2O}_{net} \frac{C^s_l}{2}; \tag{5}$$

$$J^s_{b\to l} = P^s_T C^s_b - (1 - \sigma^s) J^{H_2O}_{net} \frac{C^s_b}{2}. \tag{6}$$

Note that the net volume flow term is vectorial and the solvent drag term must then be given a sign to relate the direction of net volume flow to the direction of unidirectional tracer flux. Net water movement in the lumen-to-blood direction has been given a positive sign.

By definition, the apparent permeabilities determined from unidirectional tracer flux measurements ($P^s_{l\to b}$ and $P^s_{b\to l}$) are:

$$P^s_{l\to b} = \frac{P^s_T C^s_l + (1 - \sigma^s) J^{H_2O}_{net} \frac{C^s_l}{2}}{C^s_l}; \tag{7}$$

$$P^s_{b\to l} = \frac{P^s_T C^s_b - (1 - \sigma^s) J^{H_2O}_{net} \frac{C^s_b}{2}}{C^s_b}. \tag{8}$$

ΔP^s ($P^s_{l\to b} - P^s_{b\to l}$) can then be represented as:

$$\Delta P_s = (1 - \sigma^s) J^{H_2O}_{net} \tag{9}$$

and

$$\sigma^s = 1 - \frac{\Delta P_s}{J^{H_2O}_{net}}. \tag{10}$$

The effective pore radius can be determined from the reflection coefficient, using concepts developed by Renkin (30) and Solomon (34), with the use of the curves shown in Fig. 6 of Fordtran et al. (13).

RESULTS

Initially, we used three different sections of the gut in studies on water flux, transepithelial potential (TEP), and urea permeability. From the urea data, values for the reflection coefficients and the effective pore radii of the paracellular shunts were calculated. The reflection coefficients were calculated on the assumption that any asymmetry found in the urea permeability is due to solvent drag. The contribution of unstirred layers, if present, or solute drag cannot be

quantitatively accounted for at this time. The method of Fordtran et al. (12, 13) was used to calculate the effective pore radius. If a significant fraction of net volume flow occurs across cellular membranes, the presently reported values for pore size may be underestimated. Unstirred layers, on the other hand, would lead to an overestimation of pore size.

The data of Table I indicate that all three sections of the gut showed a net uptake, lumen to blood, of water in the control condition and each responded to the addition of 500 mM urea by a reversal of the flow, the response of all sections being of similar magnitude. The TEP showed similar changes, the largest difference being that of the colon. The P^u values are presented here for

TABLE I

*Effects of Addition of 500 mM Urea to the Luminal Perfusate on the Net Water Flux, the Transepithelial Potential, the Urea Permeabilities, the Calculated Reflection Coefficients, and Pore Size**

					Calculated	
	$J_{net}^{H_2O}$	TEP	$P_{l\to b}^u$	$P_{b\to l}^u$	σ	Pore diameter
	$\mu l/cm^2 \cdot h$	mV	$(cm^2/s) \cdot 10^5$			$\AA$
Jejunum						
Control	126±7	4.3±0.3	7.1±0.4	3.4±0.2	0.0‡	15
Experimental	−145±9	−5.3±0.3	4.1±0.4	6.2±0.6	0.59§	10
Ileum						
Control	75±6	3.0±0.2	4.6±0.2	3.1±0.2	0.31	9.0
Experimental	−102±8	−4.3±0.2	3.2±0.2	4.0±0.3	0.76‖	3.9
Colon						
Control	89±5	15.2±1.4	0.9±0.1	0.7±0.1	0.94	3.0
Experimental	−114±8	0.8±0.3	0.7±0.1	1.1±0.1	0.84	3.5

* N is 10 for all values.

Values reported by others: ‡0.0–0.2 (21); §0.5 (21); ‖1.0 (16).

they form the basis of calculations of σ and pore size. The roles of solvent and solute drag on these permeabilities are treated in the following sections. The reflection coefficients calculated for both control and hyperosmotic conditions reveal that the jejunum section showed the greater permeability (lower reflection) in the control experiments. Imposition of the 500-mM hyperosmotic solutions caused an increase in the σ's of jejunum and ileum, with a decrease in their respective calculated pore sizes. The colon responded in the opposite way in that the σ decreased slightly and the pore size increased slightly.

The reflection coefficient of 0.76 for urea (ileum) found during perfusion with 500 mM urea is significantly higher than that estimated during spontaneous water absorption. Levitt (20) and Loeschke (22, 23) have shown a similar phenomenon in the dog and frog jejunum, respectively. In the past, deviations in the theoretical reflection coefficient under these conditions have been taken to indicate permeability changes resulting from decreases in pore radius. This line of thinking has been reinforced by ultrastructural studies, which show a collapse of lateral extracellular spaces during osmotically induced volume secre-

tion (3, 22, 33). Changes in the morphology of the extracellular spaces, however, may have little bearing on the effective pore diameters at the tight junctions. There is another factor that grossly changes tracer permeability in nonbiological membrane systems and thus would influence calculated values for σ. This factor or force has been shown to be solute drag (14, 39).

These comparative tissue data led us to use the ileum as the chief tissue for the studied reported below. It was selected for study in part because of its permeability and its smaller pore size in view of our previous finding that solute drag is larger in membrane systems that have adequate permeability but smaller pore diameters.

To be able to follow the comparative roles of solvent and solute drag, it is necessary to know the direction and volume of water flow, $J_v^{H_2O}$, during control and various hyperosmotic perfusions. Table II lists data for $J_v^{H_2O}$ and TEP found during the volume flow.

TABLE II

*Effect of Addition of Urea to Luminal Perfusate on the Net Flux of Water ($J_{net}^{H_2O}$) and the Transepithelial Potential (TEP) Across the Rat Ileum**

Urea of perfusate	$J_{net}^{H_2O}$		TEP	
	Control	Experimental	Control	Experimental
mM	*μl/cm·h*		*mV*	*mV*
1	69±6	—	3.0±0.2	—
100	69±6	+1±7	3.0±0.2	+2.3±0.1
250	72±6	−56±7	3.0±0.1	−2.2±0.2
500	68±6	−93±7	3.0±0.2	−4.3±0.2

* N is 10 for all values.

In the control periods, the water flow was ~70 μl/cm·h in the direction of lumen to blood. When the electrolyte perfusate contained 100 mM urea, the $J_v^{H_2O}$ fell to ~1 μl/cm·h; when 250 mM urea was present, the volume flow was reversed to −56 μl/cm·h; at 500 mM urea, the flow was −93 μl/cm·h. These values represent changes in $J_v^{H_2O}$ of 69, 125, and 163 μl/cm·h, respectively. This volume flow response is not linear, in contrast to that found for the homopore membrane (40), which suggests that there are tissue pore changes borne out by the diffusion data below.

Labeled urea was used to evaluate the effect of solvent and solute drag upon the apparent permeability of a small tracer solute. Table III contains data regarding the tracer movement from lumen to blood and from blood to lumen. The data indicate that when only tracer amounts of urea were present in the luminal perfusate, $P^{u}_{l\to b}$ was 4.1 $cm^2/s \cdot 1 \times 10^5$, while $P^{u}_{b\to l}$ was only 2.8 $cm^2/s \cdot 1 \times 10^5$. As shown in Table II, during control perfusion, $J^{H_2O}_{l\to b}$ was ~70 μl/cm·h. The movement of urea from lumen to blood was thus accompanied by a corresponding net movement of solvent in the same direction. In terms of our previous findings (40), it is to be expected that the $P^{u}_{l\to b}$ was increased by the inward flow of water (solvent drag), as was shown by Hakim and Lifsen in dog

intestinal mucosa (17). The opposite effect is to be expected for $P^{u}_{b\to l}$, for here the diffusion of tracer urea is in a direction against the inward net flow of water. As shown before (40), it is to be expected that the P value will be something less than its simple diffusional value. The two P values above result in a tracer flux ratio of 1.46.

Confirmation of the effect of solvent drag on the apparent permeability values of urea is given by the experiments with 100 mM urea perfusate. When the perfusate contained 100 mM urea, the net $J_v^{H_2O}$ was at a minimum value (Table I). Here, with essentially no net $J_v^{H_2O}$, $P^{u}_{l\to b}$ and $P^{u}_{b\to l}$ were identical, namely 3.2, which leads to a flux ratio of 1.0. It appears, then, that under the condition of minimal $J_{net}^{H_2O}$, tracer urea diffused in both directions at similar rates. The

TABLE III

*Effect of the Addition of Urea to the Luminal Perfusate on the Apparent Permeability of Urea P^u Across the Rat Ileum**

Urea of perfusate‡	$P^{u}_{l\to b}$	$P^{u}_{b\to l}$	Tracer flux ratio: $P^{u}_{l\to b}/P^{u}_{b\to l}$
mM		$(cm^2/s)\cdot 10^5$	
1	4.1±0.2	2.8±0.1 (S)§	1.46
100	3.2±0.2	3.2±0.2 (NS)	1.0
250	3.1±0.2	3.4±0.2 (S)	0.91
500	2.9±0.1	3.6±0.2 (S)	0.81

* N is 5 for all values.

‡ Each experiment had its own control period. $P^{u}_{l\to b}$ values were 4.1 ± 0.2, 4.0 ± 0.2, and 4.2 ± 0.2, and $P^{u}_{b\to l}$ were 2.8 ± 0.1, 2.7 ± 0.2, and 2.8 ± 0.2, respectively.

§ S, significant difference: $P < 0.05$; NS, not significant: $P > 0.05$.

experiments with 250 and 500 mM urea show the expected effects of the $J_{vnet}^{H_2O}$ flow. The direction of water movement is now blood to lumen, and $P^{u}_{l\to b}$ decreases to 3.1 and 2.9. The $P^{u}_{b\to l}$ diffusion is now in the direction of the induced solvent flow, and the P^u values increase to 3.2 and 3.6. Thus far, the volume flows and tracer permeabilities qualitatively bear out the principles of solvent drag elucidated earlier on the model membrane system (32). It would be of interest to be able to describe this role of solvent drag on a quantitative basis. Since neither the recorded volume flows nor permeabilities show changes that are linear, such quantitative descriptions are difficult and the role for solute drag is obscured by the solvent drag forces.

However, as we have shown (40), it is possible to appreciate the presence of the two drag forces in the same system by considering the effects of the two forces operating simultaneously. In one case, the two forces can act together to create an effect on tracer permeability that is greater than either force working alone. In the other case, the positive effect of one drag force can be lessened, nullified, or reversed by the second drag force.

The interplay of the drag forces can be visualized with reference to Fig. 1, where the P^u values in both directions are plotted against the experimental urea

concentrations. The solid lines represent $P^{u}_{l\to b}$ and $P^{u}_{b\to l}$ (data are from Tables II and III). The broken lines represent the potential or possible effect of solvent drag upon $P^{u}_{l\to b}$ and $P^{u}_{b\to l}$. The exact position of the lines is not important and their indicated deviation from linearity is deliberate. Consider the observed $P^{u}_{b\to l}$ at 1 mM urea. The $P^{u}_{b\to l}$ increased to the value shown at the intercept of 100 mM (where the flux ratio is 1.0). Since this increase is due to the lesser effect of $J_v^{H_2O}$, one would expect increasingly large values for $P^{u}_{b\to l}$, as the solvent flow is now aided by the diffusion of urea from blood to lumen. This expected increase is represented by the upper dotted line. Because of solute drag, the increase was not realized experimentally, as is shown by the second line from the top of the figure. The differences between "expected" and observed are shown

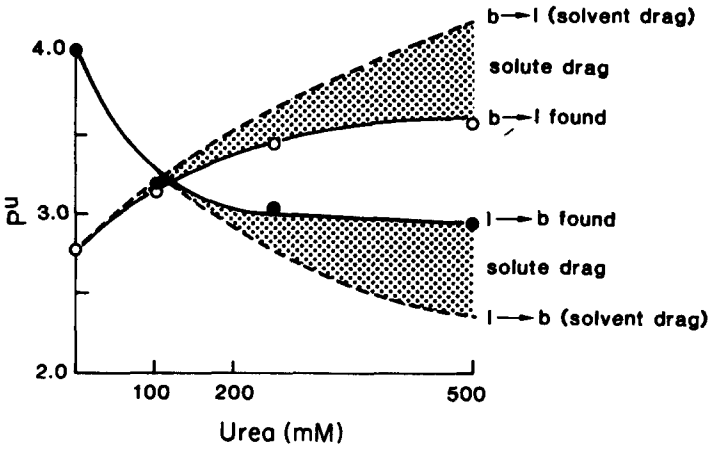

FIGURE 1. The solid lines present data, plotted from data in Table II, which show the effect of added driver urea on the permeability of tracer urea. The broken lines represent the possible P^{u} values expected from the solvent drag effect alone. The dotted area approximates the positive and/or negative effect of solute drag upon the solvent drag mechanism.

by the dotted area and approximate the magnitude of solute drag in the lumen-to-blood direction opposing the effect of solvent drag in the blood-to-lumen direction.

A similar effect is shown by the lower pair of lines. The lowest line, illustrating potential or expected $P^{u}_{l\to b}$, represents values that are greater than those found experimentally. In this instance, the diffusion of tracer urea in the direction of lumen to blood is aided by solute drag, but is lessened by the net volume flow in the opposite direction (blood to lumen). Again, the shaded area depicts the effect of solute drag.

A rough quantitative concept of the magnitude of these two drag effects is afforded by the shapes of the lines in Fig. 1 and by the amount of deviation of the flux ratios listed in Table III.

Physical forces other than solute and solvent drag could influence the changes in P values. A decrease in pore diameter with an increase in the reflection coefficient should result in a decrease in both $P^{u}_{l\to b}$ and $P^{u}_{b\to l}$. However, we found

a decrease in $P^{u}_{b\to l}$ and an increase in $P^{u}_{l\to b}$. As stated above, the changes are compatible with the effects of solute drag, even though the pore size may have changed. An additional physical effect is related to the presence of unstirred layers. It is to be expected that an unstirred layer would decrease $P^{u}_{l\to b}$ and increase $P^{u}_{b\to l}$. The experimental findings, however, are just the opposite, which suggests that solute drag has minimized or masked a possible unstirred layer effect.

The data to this point implicate solute drag as a force influencing the diffusion and permeability characteristics of a tracer solute. The magnitude of the effect is seen to be dependent on the driver solute concentration, as was shown previously in model systems (16, 40). Several other salient characteristics of the solute drag dogma are testable. Solute drag was seen to be increased when the tracer solute and/or the driver solute was increased in size.

The first of these characteristics was tested by the use of erythritol as the tracer (driven) solute. Table IV lists the results. In these studies, 500 mM urea was used as the driver solute.

TABLE IV

*Effect of Addition of 500 mM Urea to the Luminal Perfusate on the Apparent Permeability of Urea P^{u} and Erythritol P^{e} Across the Rat Ileum**

Tracer	$P_{l\to b}$		Control/experimental	$P_{b\to l}$		Control/experimental
	Control	Experimental		Control	Experimental	
	$(cm^2/s)\cdot 10^5$			$(cm^2/s)\cdot 10^5$		
Urea	4.2±0.2	2.9±0.1 (S)‡	0.6	2.8±0.2	3.6±0.2 (S)	1.3
Erythritol	2.3±0.2	1.6±0.2 (S)	0.7	1.3±0.1	1.8±0.2 (S)	1.4

* N is 5 for all values.

‡ S, significant difference: $P < 0.05$.

As indicated in Table IV, the P^{e} values are less than P^{u}, as is to be expected from a tracer solute of twice the molecular weight (122 vs. 60). The driver solute (500 mM urea) had slightly larger effects on the bidirectional permeabilities of erythritol, as is shown by the flux ratios even though the basic permeability of erythritol is lower than that of urea. In previous studies on nonbiological membranes (16), it was possible to vary the tracer solute size over a 27-fold range (180–5,000 mol wt), and in such a system a graded series of flux ratios resulted, which further illustrates the effect of tracer size. The present study of the two tracer solutes is in agreement with anticipated results.

The second characteristic, the role of driver solute size (molecular weight), was evaluated in studies in which urea, mannitol, and PEG 600 were each used as the hyperosmotic solute at a concentration of 500 mM. $J^{H_2O}_{net}$ and TEP were measured in each experiment. Each of the three hyperosmotic agents caused similar changes in $J^{H_2O}_{net}$ and TEP, as shown in Table V.

The comparative solute drag effects of the three hyperosmotic agents are shown in Table VI. It is clear that the three agents caused similar changes in both $P^{u}_{l\to b}$ and $P^{u}_{b\to l}$, in spite of the large differences in molecular weight and the

TABLE V

*Effect of Addition of 500 mM Urea, Mannitol, or PEG 600 to the Luminal Perfusate on the Net Flux of Water ($J_{net}^{H_2O}$) and the Transepithelial Potential Difference (TEP) Across the Rat Ileum**

Hyperosmotic driver	$J_{net}^{H_2O}$		TEP	
	Control period	Experimental period	Control period	Experimental period
	$\mu l/cm \cdot h$		mV	
500 mM urea	68±6	−93±7	3.0±0.2	−4.3±0.2
500 mM mannitol	71±5	−86±7	3.1±0.2	−4.4±0.3
500 mM PEG 600	67±5	−88±8	2.9±0.2	−4.0±0.4

* N is 10 for all values.

corresponding large differences in the permeabilities of the driver solutes. The 3-fold increase in the weight of urea as compared with mannitol is accompanied by a 16-fold decrease in the permeability of mannitol as compared with urea. In spite of this large decrease in the pore flux of mannitol to act as a driver, its larger size allowed it to influence both $P^u_{l\to b}$ and $P^u_{b\to l}$ as effectively as the more permeable solute urea. That is, the lower flux of mannitol was as effective as the greater flux of urea.

Similar reasoning can be used with the data obtained with PEG 600, but in this case, a similar quantitative comparison is not possible. With the various molecular sizes present in PEG 600 (the molecular group of solutes having an average molecular weight of 600), the resultant changes in $P^u_{l\to b}$ and $P^u_{b\to l}$ will reflect the cumulative effect of the average of each of the solute sizes, permeabilities, and concentrations. Since it is likely that even the smaller species of PEG 600 have permeabilities much smaller than mannitol (see reference 40 for a comparison) and the larger species may be essentially impermeable, the ability

TABLE VI

*Effects of Increasing Size of Driver Solutes upon the Apparent Permeability of Tracer Urea Across the Rat Ileum**

Hyperosmotic solute‡	$P^u_{l\to b}$		$P^u_{b\to l}$		Experimental flux ratios: $P^u_{l\to b}/P^u_{b\to l}$
	Control	Experimental	Control	Experimental	
	$(cm^2/s)\cdot 10^5$		$(cm^2/s)\cdot 10^5$		
Urea	4.2±0.2	2.9±0.1 (S)§	2.8±0.2	3.6±0.2 (S)	0.81
Mannitol	4.1±0.3	3.0±0.1 (S)	2.8±0.1	3.4±0.2 (S)	0.88
PEG 600	4.0±0.2	2.3±0.2 (S)	2.8±0.2	3.6±0.2 (S)	0.64

* N is 5 for all values.

‡ Solutes were used at 500 mM concentration. Urea has a molecular weight of 60 and a $P^u_{l\to b}$ of 4.1×10^{-5} cm²/s. Mannitol has a molecular weight of 180 and a $P^m_{l\to b}$ of 0.28×10^{-5} cm²/s. PEG 600 is a mixture of molecular sizes with an average molecular weight of 600. Data are not available for $P^{PEG\ 600}$.

§ S, significant difference: $P < 0.05$.

of this driver solute to induce solute drag further confirms that increased driver size aids solute-solute interaction in this biological tissue, just as it does in model homopore and heteropore membranes (16).

An additional reason for including the data on the "mixed solute" PEG 600 is its potential role as a model of the mixed solutes present in the lumen of the gut during the digestion and absorption of a wide variety of mixed foods.

DISCUSSION

Franz and Van Bruggen's original finding (15) of tracer solute flux asymmetry was made during the course of studies on frog skin Na^+ transport. The observed asymmetry of the fluxes was shown to be unrelated to the presence of biological processes such as Na transport (2). This was confirmed by the demonstration of similar findings on a nonbiological membrane (14). The nonbiological membrane work was expanded to include studies in which the parameters of membrane pore size, concentration of hyperosmotic agent, and molecular size of the hyperosmotic agent or the tracer solute were varied. It was found (16) that solute-solute interaction, within pore confines, led to increases or decreases in the permeabilities of tracers, depending upon the transmembrane direction of the flow of the permeable hyperosmotic agent. It was also found that the larger hyperosmotic agents exerted a greater effect and that the larger tracer solutes were more affected. In these studies with frog skin and nonbiological heteroporous membranes, it was shown that the solute diffusion being studied was occurring through pores of widely differing diameters and along tortuous diffusion channels. Others had suggested (28, 35–37) that in such membranes, mechanisms other than solute drag might explain the solute flux asymmetry. It became possible to use homoporous membranes and to compare findings on them with heteroporous membranes. The concept of interaction coefficients was introduced (16) and the studies confirmed the concept that transmembrane solute drag is the result of a kinetic and frictional interaction of driver and tracer solutes.

In past studies, the comparative roles of solvent drag and solute drag, even on nonbiological membranes, were not elucidated. Since solute drag induced by hyperosmotic solutions also causes solvent drag, it became necessary to separate and systematize these effects. This was done on model heteropore and homopore membranes with a variety of solutes (35).

The next logical development related to the concept of solute drag was to apply the principles to biological systems and attempt to determine whether solute drag was operative in biological transmembrane processes. The gastrointestinal tract was selected as a system of membranes penetrated by shunt pathways (6, 31, 41) that had tight junctions and lateral extracellular spaces (24, 25, 42), which allowed the diffusion of small solutes through "pores" sufficiently narrow to permit solute-solute interaction. Segments of gut might be considered similar to the model membranes in our studies in which the membrane barrier separated two main compartments. Here the two compartments are the lumen of the gut and the vascular system.

We hoped that nonelectrolyte solutes could be chosen that might diffuse between the two compartments purely by physical means and without the participation of transmembrane biological transport mechanisms. Such a diffusion from lumen to blood and vice versa might then be described by a general diffusion equation (16), which relates three of the known forces that effect the diffusion of electrically neutral solutes:

$$\text{Net flow of tracer} = \text{self diffusion} \pm \text{solvent drag} \pm \text{solute drag.}$$

$$\underset{\text{diffusion}}{\text{Self-}} \qquad \underset{\text{Solvent}}{\text{Drag}} \qquad \underset{\text{Solute}}{}$$

$$J^s_T = P_{TT}\Delta C_T \pm \bar{C}_T(1 - \sigma)_T J_v \pm P_{TD}\Delta C_D.$$

Here J^s_T, the net flow of tracer solute, is seen to be the result or summation of the effects of self-diffusion and the positive or negative effects of solvent drag and solute drag (39, 40).

It is acknowledged that this summation of three recognized forces is probably oversimplified, considering the complex nature of the contents of the two compartments (gut lumen and the blood), the involved interaction between the multiple solutes, and the modifying effects of each of the three cited forces upon each other. In spite of the obvious problems of the experimental approach to biological transport, the present studies were completed in the hope that they might indicate an as yet undocumented role for the solute drag mechanism as a force in biological membrane transport.

The experiments described in Table I illustrate a number of principles or forces that are involved in normal (control) gut absorption. They also illustrate the profound physiological changes that occur when the bathing solution is made hyperosmotic. The net flux of water, $J^{H_2O}_{net}$, is seen to be in an inward or lumen-to-blood direction when the bathing solutions of all three segments of gut were perfused with isosmotic electrolyte. Under this "normal" condition, the summation of electrolyte effects yields a positive membrane potential. The nonelectrolyte, 1 mM tracer urea, is seen to have a permeability asymmetry for $P_{l\to b} > P_{b\to l}$ in all three segments. Since urea moves across the lumen-blood barrier by diffusion, the asymmetry found in the permeability values for urea is attributed to the effects of solvent drag. With the net inward flow of water, $P^u_{l\to b}$ is expected to be larger than its base value and $P^u_{b\to l}$ is expected to be lower because of the opposing flow of water. These expectations are realized with each gut segment. These findings appear to bear out the presence and functional role of the solvent drag mechanism. In this mechanism, the net solvent movement interacts with dissolved diffusing solute to increase or decrease its measured diffusion rate. In a previous paper (40), we discussed the basic similarities between the physical forces presently labeled "solvent drag" and "solute drag" and suggested that the molecular level collisions of solvent(s) and solute(s) have a commonality in both of the drag forces.

When a hyperosmotic solution of a permeable solute is introduced into the system as the luminal perfusate, profound effects are seen. The direction of the net volume flow is changed to an outward (blood to lumen) flow and the volume

flow elicited by the 500-mM hyperosmotic solution is larger than the control inward flow. These changes in $J_{net}^{H_2O}$ are accompanied by changes in the transepithelial potentials. For jejunum and ileum, the membrane potential was reversed, and with the colon, the size of the positive charge was reduced in a similar manner.

In keeping with the previous discussion, the change in $J_{net}^{H_2O}$ resulted in not unexpected changes in tracer permeabilities. All the values for $P_{l\to b}^{u}$ decreased (opposing solvent flow) and those for $P_{b\to l}^{u}$ increased (assisting solvent flow). The amount of change in net volume flow, the resultant changes in TEP, and the permeability values are a function of the concentration of the hyperosmotic solution and the degree of transepithelial permeability of the hyperosmotic agent itself.

The data presented in Tables II and III illustrate the involvement of the concentration of the hyperosmotic solution and show its effect on both solvent movement and the interaction of diffusing driver and tracer solutes, solute drag. The effects of the hyperosmotic solutions upon the permeabilities of tracer urea are shown in Fig. 1 as a function of the concentration of the hyperosmotic agent. A similar plot can be made for the permeability changes as a function of the elicited solvent flow. In relating volume flow and driver solute concentration, the role of each of these forces must be compared but distinguished from each other. As the concentration of the hyperosmotic agent is increased, two effects upon tracer permeability are seen. There will be the usual flow of solvent into the hyperosmotic agent compartment. This solvent flow will cause an increase in the diffusion of tracer in the same direction as the solvent flow, but it will decrease the rate of tracer solute diffusion in the opposite direction. The magnitude of these effects will be dependent upon the volume of solvent flow, and this volume of flow is proportional to the concentration of the hyperosmotic solution. The second effect of the hyperosmotic agent will be to impose the effect of solute drag upon the diffusion of the tracer. This drag effect will occur because the hyperosmotic solute itself is a permeable solute and will flow down its concentration gradient. The flux of the hyperosmotic solute is proportional to its permeability and to its concentration. The magnitude of interaction between the flux of hyperosmotic agent (driver) and the tracer solute is concentration dependent (16).

The solute drag effect may now be considered together with the solvent drag effect. When tracer solute is diffusing into the hyperosmotic compartment, it is aided by the flow of solvent in the same direction. Its accelerated diffusion is, however, lessened by the interaction with driver solute. The net effect of these two directional forces will generally result in some positive or negative effect upon the measured permeability of the tracer solute. When the two opposing forces are of about the same magnitude, there may be little change in the apparent permeability of the tracer. Fig. 1 illustrates the various combinations of the two forces and the various results that may be obtained.

It is possible to describe this interaction of forces in the simple manner cited above only when the membrane system and its perfusion fluids have been simplified to represent a model system. When the concepts of solvent and solute

drag are applied to an intact biological system having bidirectional solute flows with periods of hyperosmolarity and solvent flow variation, the potential multiple interactions of solutes and solvent make it apparent that a most dynamic condition is present even during the operation of the mechanism of passive or simple diffusion.

The solute-solute interaction described above is also modifiable by the other two principles to be considered in the concept of solute drag. Each relates to the "size" of the solute species being studied. The larger the tracer solute, the greater is the effect of the driver solute. Similarly, the larger the driver solute, the greater is its effectiveness as a driver.

When erythritol was used as the tracer solute, it showed the expected lower permeability, but was affected by the driver urea solute to about the same degree as was the smaller tracer urea.

In a similar way, the use of the larger driver solutes mannitol and PEG 600, with their known lower permeabilities, indicate that the larger driver solutes, even with their greatly lowered permeabilities, were able to be effective driver solutes.

In conclusion, these studies on rat intestine appear to document the need for consideration of the probable role of solute drag in biological systems. However, the joint participation of the two drag forces, solvent and solute drag, should be considered in quantitative descriptions of biological transport.

Original version received 13 December 1983 and accepted version received 29 October 1984.

REFERENCES

1. Altamirano, M. 1969. Action of concentrated solutions of nonelectrolytes on the dog gastric mucosa. *Am. J. Physiol.* 216:33–40.
2. Anderson, B., and H. H. Ussing. 1957. Solvent drag of non-electrolytes during osmotic flow through isolated toad skin and its response to antidiuretic hormone. *Acta Physiol. Scand.* 39:228–239.
3. Bentzel, C. J., B. Parisa, and D. K. Hare. 1969. Osmotic flow across proximal tubule of *Necturus*: correlation of physiologic and anatomic studies. *Am. J. Physiol.* 217:570–580.
4. Biber, T. U. L., and P. F. Curran. 1968. Coupled solute fluxes in toad skin. *J. Gen. Physiol.* 51:606–620.
5. Bihler, I., K. A. Hawkins, and R. K. Crane. 1962. Studies on the mechanism of intestinal absorption of sugars. VI. The specificity and other properties of Na^+ dependence entrance of sugars into intestinal tissue under anaerobic conditions in vitro. *Biochem. Biophys. Acta.* 59:94–102.
6. Boulpaep, E. L., and J. F. Seely. 1971. Electrophysiology of proximal and distal tubules in the autoperfused dog kidney. *Am. J. Physiol.* 221:1084–1096.
7. Curran, P. F., S. G. Schultz, R. A. Chez, and R. E. Fuisz. 1967. Kinetic relations of the Na-amino acid interaction at the mucosal border of intestine. *J. Gen. Physiol.* 50:1261–1286.
8. Curran, P. F., and A. K. Solomon. 1957. Ion and water fluxes in the ileum of rats. *J. Gen. Physiol.* 41:143–168.
9. Dainty, J., and C. R. House. 1966. 'Unstirred layers' in frog skin. *J. Physiol. (Lond.).* 182:66–78.

10. Diamond, J. M. 1977. The epithelial junction: bridge, gate and fence. *Physiologist.* 20:10–18.

11. Diamond, J. M., and W. H. Bossert. 1967. Standing-gradient osmotic flow. A mechanism for coupling of water and solute transport in epithelia. *J. Gen. Physiol.* 50:2061–2083.

12. Fordtran, J. S., F. C. Rector, and N. W. Carter. 1968. The mechanisms of sodium absorption in the human small intestine. *J. Clin. Invest.* 47:884–900.

13. Fordtran, J. S., F. C. Rector, M. F. Ewton, N. Soter, and J. Kinney. 1965. Permeability characteristics of the human small intestine. *J. Clin. Invest.* 44:1935–1944.

14. Franz, T. J., W. R. Galey, and J. T. Van Bruggen. 1968. Further observations on asymmetrical solute movement across membranes. *J. Gen. Physiol.* 51:1–12.

15. Franz, T. J., and J. T. Van Bruggen. 1967. Hyperosmolarity and the net transport of nonelectrolytes in frog skin. *J. Gen. Physiol.* 50:933–949.

16. Galey, W. R., and J. T Van Bruggen. 1970. The coupling of solute fluxes in membranes. *J. Gen. Physiol.* 55:220–242.

17. Hakim, A. A., and N. Lifsen. 1964. Urea transport across dog intestinal mucosa in vitro. *Am. J. Physiol.* 206:1315–1320.

18. Humphreys, M. H. 1976. Inhibition of NaCl absorption from perfused rat ileum by furosemide. *Am. J. Physiol.* 230:1517–1523.

19. Kedem, O., and A. Katchalsky. 1958. Thermodynamic analysis of the permeability of biological membranes to nonelectrolytes. *Biochem. Biophys. Acta.* 27:224–246.

20. Levitt, D. G., A. A. Hakim, and N. Lifson. 1969. Evaluation of components of transport of sugars by dog jejunum in vivo. *Am. J. Physiol.* 217:777–783.

21. Lief, P. D., and A. Essig. 1973. Urea transport in the toad bladder; coupling of urea flows. *J. Membr. Biol.* 12:159–176.

22. Loeschke, L., C. J. Bentzel, and T. Z. Csaky. 1970. Asymmetry of osmotic flow in frog intestine: functional and structural correlation. *Am. J. Physiol.* 281:1723–1731.

23. Loeschke, L., D. Hare, and T. Z. Csaky. 1971. Passive sugar fluxes across frog jejunum in vitro. *Pflügers Arch. Eur. J. Physiol.* 328:1–20.

24. Machen, T. E., D. Erlij, and F. B. P. Wooding. 1972. Permeable junctional complexes: the movement of lanthanum across rabbit gallbladder and intestine. *J. Cell Biol.* 54:302–312.

25. Martinez-Palomo, A., and D. Erlij. 1973. The distribution of lanthanum in tight junctions of the kidney tubule. *Pflügers Arch. Eur. J. Physiol.* 343:267–272.

26. Murakami, M., M. Saito, and M. Suda. 1977. Contribution of diffusive pathway in intestinal absorption of glucose in rat under normal feeding condition. *Experientia.* 33:1469–1470.

27. Nellans, H. N., R. A. Frizzell, and S. G. Schultz. 1973. Coupled sodium-chloride influx across the brush border of rabbit ileum. *Am. J. Physiol.* 225:467–475.

28. Patlak, C. S., and S. I. Rapoport. 1971. Theoretical analysis of net tracer flux due to volume circulation in a membrane with pores of different sizes. Relation to the solute drag model. *J. Gen. Physiol.* 57:113–124.

29. Quay, J. F., and W. M. Armstrong. 1969. Sodium and chloride transport by isolated bullfrog small intestine. *Am. J. Physiol.* 217:694–702.

30. Renkin, E. M. 1954. Filtration, diffusion, and molecular sieving through porous cellulose membranes. *J. Gen. Physiol.* 38:225–243.

31. Rose, R. C., and S. G. Schultz. 1971. Studies on the electrical potential profile across

rabbit ileum; effects of sugars and amino acids on transmural and transmucosal electrical potential differences. *J. Gen. Physiol.* 57:639–663.

32. Schultz, S. G., R. A. Frizzel, and H. N. Nellans. 1974. Ion transport by mammalian small intestine. *Annu. Rev. Physiol.* 36:51–91.
33. Smulders, A. P., J. M. Tormey, and E. M. Wright. 1972. The effect of osmotically induced water flows on the permeability and ultrastructure of the rabbit gallbladder. *J. Membr. Biol.* 7:164–197.
34. Solomon, A. K. 1960. Measurements of the equivalent pore radius in cell membranes. *In* Membrane Transport and Metabolism. A. Kleinzeller and A. Kotyk, editors. Academic Press, Inc., New York. 94–113.
35. Stender, S., K. Kristensen, and E. Skadhauge. 1973. Solvent drag by solute-linked water flow: a theoretical examination. *J. Membr. Biol.* 11:377–398.
36. Ussing, H. H. 1966. Anomalous transport of electrolytes and sucrose through the isolated frog skin induced by hypertonicity of the outside bathing solution. *Ann. NY Acad. Sci.* 137:543–555.
37. Ussing, H. H., and B. Johansen. 1969. Anomalous transport of sucrose and urea in toad skin. *Nephron.* 6:317–328.
38. Ussing, H. H., and E. E. Windhager. 1964. Nature of shunt path and active sodium transport path through frog skin epithelium. *Acta Physiol. Scand.* 61:484–504.
39. Van Bruggen, J. T., J. D. Boyett, A. L. Van Bueren, and W. R. Galey. 1974. Solute flux coupling in a homopore membrane. *J. Gen. Physiol.* 63:639–656.
40. Van Bruggen, J. T., B. Chalmers, and M. Muller. 1982. Effects of solvent and solute drag on transmembrane diffusion. *J. Gen. Physiol.* 79:507–528.
41. White, J. F., and W. M. Armstrong. 1971. Effect of transport solutes on membrane potentials in bullfrog small intestine. *Am. J. Physiol.* 221:194–201.
42. Whittembury, G., and F. A. Rawlins. 1971. Evidence for a paracellular pathway for ion flow in the kidney proximal tubule: electronmicroscopic demonstration of lanthanum precipitate in the tight junction. *Pflügers Arch. Eur. J. Physiol.* 330:302–309.
43. Wright, E. M., A. P. Smulders, and J. M. Tormey. 1972. The role of the lateral intercellular spaces and solute polarization effects on the passive flow of water across the rabbit gallbladder. *J. Membr. Biol.* 7:198–219.